FREQUENCY BIASES ASSOCIATED WITH DISTRIBUTED CAVITY PHASE AND MICROWAVE LEAKAGE IN THE ATOMIC FOUNTAIN PRIMARY FREQUENCY STANDARDS IEN-CSF1 AND NIST-F1†

S.R. Jefferts, J.H. Shirley, N. Ashby, T.P. Heavner, E.A. Donley
NIST –Time and Frequency Division,
325 Broadway
Boulder , CO USA 80305

F. Levi
Istituto Elettrotecnico Nazionale – Torino IT

E.A. Burt, G. J. Dick
Jet Propulsion Laboratories, Pasadena, CA USA

ABSTRACT†

We show that the frequency bias caused by distributed cavity phase has a strong dependence on microwave power. We also show that frequency biases associated with microwave leakage have distinct signatures in their dependence on microwave power and the physical location of the leakage interaction with the atom.

1. INTRODUCTION

The subject of frequency shifts in atomic frequency standards caused either by distributed cavity phase or microwave leakage goes back to the earliest days of the thermal beam standards [1,2], and has been the subject of continuing theoretical and experimental work over the last fifty years. [3-8]. Laser-cooled fountain frequency standards pose problems with respect to both distributed cavity phase and microwave leakage different from those associated with thermal beam standards. This is due both to the very different microwave structure used in fountains as well as the low center-of-mass velocity and very narrow velocity distribution, which allows operation at significantly elevated microwave power in fountain standards.

We discuss the dependence on microwave power of the frequency biases induced in an atomic fountain by the distributed cavity phase (DCP) and microwave leakage. The entire discussion takes place within the limit of small detuning because the velocity of the atoms, typically a maximum of 3m/s, results in a maximum Doppler shift of only 100 Hz.

The analysis of the phase of the microwave field within the typically TE_{011}, microwave cavities used in cold-atom fountain frequency standards has been the subject of a large body of work. DeMarchi provided the seminal contributions of proving a correspondence between the phase and power-flows within the microwave cavity, identifying the preferred cavity configuration and modeling the phase of the microwave field within the cavity [9-11]. Three-dimensional analyses of the microwave field within the cavity have been completed by several authors [12-16]. In many of these studies large phase excursions are predicted. At least one author has used these phase excursions to predict frequency shifts in the $\delta f/f \simeq 10^{-16}$ range as a result of distributed cavity phase [14], larger than the current value assigned in the error budget of many operational fountain type primary frequency standards. We note that the theory presented here allows one to test that prediction.

We begin by briefly reviewing the properties of the microwave field and within a resonant TE_{011} cavity. We then solve the Schrödinger equation for a two-level atom in the case where the field within the microwave cavity has both real and imaginary parts, which is the case required to understand both the distributed cavity phase frequency shift and the microwave leakage frequency shift. We then examine the dependence on microwave field amplitude of the frequency bias caused either by distributed cavity phase or microwave leakage.

2. MICROWAVE CAVITIES AND PHASE

The typical microwave cavity used in cesium (and rubidium) fountain frequency standards is a cylindrical cavity resonating in the TE_{011} mode at the hyperfine frequency of the atom, 9.193 GHz in the case of cesium. See Fig. 1. The "z-axis" of the cavity is aligned with the gradient of the gravitational potential and atoms enter and leave the cavity via below-cutoff waveguides. This cavity has the crucial property of allowing relatively large diameter ($2r_a \sim$ 1cm at ν_0 = 9.2 GHz.) cylindrical waveguides for atoms to enter and leave the cavity without unduly influencing the TE_{011} mode of the cavity and thereby causing large phase gradients in the microwave field [10]. To lowest order the field within the cavity is describable as purely TE ($E_Z \equiv 0$) and all field components are derivable from the longitudinal magnetic field $H_z(x,y)$ [17]. Under these assumptions and using a trivial extention of the notation of DeMarchi in [11], the longitudinal field can be written as

$$H_Z(x,y,z) = |H(x,y)| e^{i\varphi(x,y)} f(z)\hat{z}, \quad (1)$$

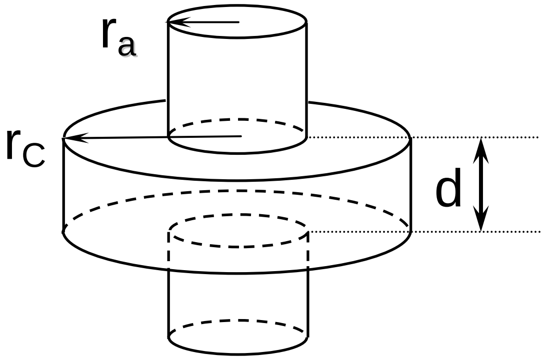

Figure 1. A schematic diagram of the TE_{011} microwave cavity used in most cesium fountain frequency standards.

where $\varphi(\mathrm{x},\mathrm{y})$ is the distributed cavity phase under discussion here. The expression for the real part of the field within the cavity is given (with a change to cylindrical coordinates ρ,ϕ and z) to lowest order by

$$\mathrm{H_Z}(\rho,\phi,\mathrm{z})=\left(\frac{\pi}{2}\right)\mathrm{H_0 J_0}\left(\frac{\mathrm{p}'_{0,1}\rho}{\mathrm{r_c}}\right)\sin\left(\frac{\pi \mathrm{z}}{\mathrm{d}}\right), \quad (2)$$

where $\mathrm{J_n}$ is the $\mathrm{n^{th}}$ Bessel function and $\mathrm{p}'_{n,m}$ is defined as the $\mathrm{m^{th}}$ solution of $\frac{\mathrm{dJ_n(x)}}{\mathrm{dx}}=0$, $\mathrm{r_c}$ is the radius of the cavity, d is the height of the cavity, and $\pi H_0/2$ is the field amplitude at the center of the cavity (see Fig. 1 and [17]). The cavity phase is defined by the relation

$$\varphi \equiv \tan^{-1}\left(\frac{\mathrm{Im}(\mathrm{H_Z})}{\mathrm{Re}(\mathrm{H_Z})}\right), \qquad (3)$$

where the real part of H is approximated by Eq (2) and the imaginary part is, roughly, approximated by

$$\mathrm{Im}(\mathrm{H_z})=\frac{\pi\mathrm{H_0}}{2\mathrm{Q}}\left[\left(1+\left(\frac{\rho}{\mathrm{r_c}}\right)^2+\left(\frac{\rho}{\mathrm{r_c}}\right)^4\cos 4\phi\right)\left(\frac{\mathrm{z}}{\mathrm{d}}-\frac{1}{2}\right)^2\right]. \quad (4)$$

Here Q is the quality factor of the cavity. The second term in Eq. (4) comes from power flow to the walls from the standing mode of the field, and the third term comes from power flow associated with the four-feed structure of the particular cavity investigated here [12]. The terms proportional to $\frac{\rho}{r_c}$ and $\frac{\mathrm{z}}{\mathrm{d}}$ are negligible for a symmetric, well constructed cavity and are not included here. The overall cavity phase has been set equal to zero at the geometric center of the cavity.

Several things can be seen by inspection of the previous equations. First, the phase of the microwave field within the cavity is independent of microwave power (as it should be). The effect on the atom of the imaginary part of $\mathrm{H_z}$ is, however, unlikely to be independent of microwave power. Second, the microwave phase can become relatively large when the real part of $\mathrm{H_z}$ is sufficiently small, or equivalently, the Rabi frequency of the atom is sufficiently small. What is ultimately of interest is not the value of the phase angle of the microwave field, but rather the value of the phase angle imposed on the atomic wave function, and any resulting frequency biases. In order to quantify the effect of the imaginary part of the microwave field upon the atom, we now obtain a solution to the time-dependent Schrödinger equation as the atoms pass through a cavity with fields described by Eq. (2) & (4).

3. SCHRÖDINGER EQUATION AND RAMSEY LINESHAPES

We extensively employ the theoretical framework developed by Shirley [18-20] and present here the extensions required to handle both the real and imaginary phases of microwave field.

The Hamiltonian for the system can be written as (cf. (7) of [20])

$$\mathcal{H}=\hbar\begin{pmatrix}\omega_a & 2\mathrm{b}\cos\omega \mathrm{t}+2\mathrm{b}'\sin\omega \mathrm{t}\\ 2\mathrm{b}\cos\omega \mathrm{t}+2\mathrm{b}'\sin\omega \mathrm{t} & \omega_b\end{pmatrix}, \quad (5)$$

where $\hbar\omega_a$ and $\hbar\omega_b$ are respectively the energies of the upper and lower states. The interaction Rabi frequency for the real part of the microwave field is given by $2\mathrm{b}=\mu_B g\,\mathrm{Re}(\mathrm{H_Z})/\hbar$, where μ_B is the Bohr magneton, g the Landé g-factor and H_Z the microwave magnetic field parallel to the quantization axis imposed by the external c-field. A similar expression applies for b', $2\mathrm{b}'=\mu_B g\,\mathrm{Im}(\mathrm{H_Z})/\hbar$, the Rabi frequency due to the imaginary part of the microwave field. Both $\mathrm{b(t)}$ and $\mathrm{b'(t)}$ are time-dependent, owing to the atoms motion in the cavity. We also define $b_0 \equiv \frac{g\mu_B}{2\hbar}H_0$.

In the rotating wave approximation, the Hamiltonian in 1.5 is written

$$\mathcal{H}=\hbar\begin{pmatrix}\omega_a & (\mathrm{b}+i\mathrm{b}')e^{-i\omega t}\\ (\mathrm{b}-i\mathrm{b}')e^{i\omega t} & \omega_b\end{pmatrix}. \quad (6)$$

Note the sign change in $\mathrm{b'(t)}$ in the off-diagonal couplings. This comes about because the rotating wave approximation selects one exponential from $\sin\omega t$ in one coupling and the other exponential in the other coupling (Compare to (7) and (8) in [20]). Using the "phase factored" solutions, α and β, (cf (9 & 10) of [20]) gives us, finally, the Schrödinger equation for the system,

$$i\hbar\frac{\mathrm{d}}{\mathrm{dt}}\begin{pmatrix}\alpha\\ \beta\end{pmatrix}=\hbar\begin{pmatrix}-\Delta & \mathrm{b}+i\mathrm{b}'\\ \mathrm{b}-i\mathrm{b}' & \Delta\end{pmatrix}\begin{pmatrix}\alpha\\ \beta\end{pmatrix}. \quad (7)$$

With the initial condition $\alpha(0)=1$ and $\beta(0)=0$ then α is the probability amplitude that the system remains in its initial state and β the probability amplitude that the system changes state. Δ is half the detuning $\delta\omega$ from the atomic resonance ω_0: $\Delta = \frac{1}{2}(\omega-\omega_0) = \frac{\delta\omega}{2}$, where $\omega_0 = \omega_a - \omega_b$ is the hyperfine splitting of the atom. Δ, b, and b' are all real, possibly time-dependent, quantities.

We have given a solution to (7), valid through first order in Δ and b', under the assumption that the detuning is small compared to the Rabi frequency, in [21]. We quote here only the final results.

Using our solutions mentioned above and assuming that the real part of the excitation is the same for both Ramsey pulses leads to a transition probability of

$$P = \frac{\sin^2(2b_0\tau)}{2}\left[1+\cos\delta\omega T_R + \left\{\begin{matrix}(\varepsilon_2-\varepsilon_1)\csc b_0\tau + \\ (\eta_1+\eta_2)\sec b_0\tau\end{matrix}\right\}\sin\delta\omega T_R\right]. \quad (8)$$

The term $b_0\tau = \int_0^\tau b(t)\,dt$, that is, b_0 is the average value of $b(t)$ during the excitation time τ, which amounts to $\pi/4$ at optimum power, and $\varepsilon_{1,2}$ and $\eta_{1,2}$ are proportional to the imaginary part of the microwave field b'. The transition probability, P, is clearly a normal Ramsey fringe (the $\cos\delta\omega T_R$ term) plus an underlying fringe of small amplitude and $\pi/2$ displacement (the $\sin\delta\omega T_R$ term). The latter asymmetrically distorts the Ramsey curve and leads to a frequency bias. The frequency bias is proportional to the difference between the transition probabilities P_L and P_R on the left and right sides of the central Ramsey fringe at equal detunings. This difference is given by

$$P_L - P_R = \sin^2(2b_0\tau)\left[\frac{\varepsilon_2-\varepsilon_1}{\sin(b_0\tau)} + \frac{\eta_2+\eta_1}{\cos(b_0\tau)}\right], \quad (9)$$

where $P_{L,R}$ is the probability given by (8) on the left and right sides of the central Ramsey fringe respectively (that is with $\delta\omega = \mp\pi/2T_R$, respectively). Eq (9) is plotted below in Fig 2. The complicated nature of the power dependence of the frequency bias associated with distributed cavity phase is immediately apparent in Fig. 2. This signature should allow measurement of the frequency bias associated with distributed cavity phase, or at least allow the placing of an upper limit on the effect.

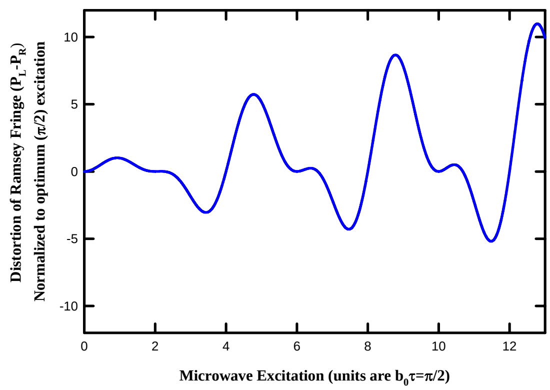

Figure 2. The distortion of the Ramsey fringe plotted caused by distributed cavity phase with respect to the microwave excitation (number of $\pi/2$ pulses). The distortion is proportional to the frequency bias and the data shown here are normalized to the shift at optimum power (one $\pi/2$ pulse).

4. MICROWAVE LEAKAGE

We can use the Hamiltonian, Eq. (6), also to investigate microwave leakage, except that in this case both b and b' are presumably small. We divide our analysis into three cases: leakage before the two Ramsey interactions, leakage between the Ramsey pulses, and leakage after the Ramsey interactions. Because the state-selection mechanism in NIST-F1 and IEN-CSF1 destroys any microwave coherence and projects the atoms into a pure F=3 state we can ignore the case of leakage before the first Ramsey interaction. We note however that the solution to the case of leakage before the first Ramsey interaction can be obtained from the case of leakage after the second Ramsey interaction by the substitution of $-t$ for t.

Some general results can be obtained [22]:

1. Microwave leakage in phase (the b term) with the field in the Ramsey cavity does not cause a frequency shift.
2. Microwave leakage in quadrature phase (the b' term) does not cause a frequency shift if it is applied symmetrically with respect to the center of the Ramsey interaction at $T_R/2$.
3. Microwave leakage in quadrature phase applied asymmetrically with respect to $T_R/2$ excites a Ramsey fringe shifted with respect to the central fringe (a $\sin(\delta\omega T_R)$ term) much like that in Eq. (8), which can cause a frequency bias.

We investigate the power dependence of these frequency biases next. Full solutions to the Schrödinger Equation for all three leakage cases are given in [22]. The various specific cases of microwave leakage are examined below.

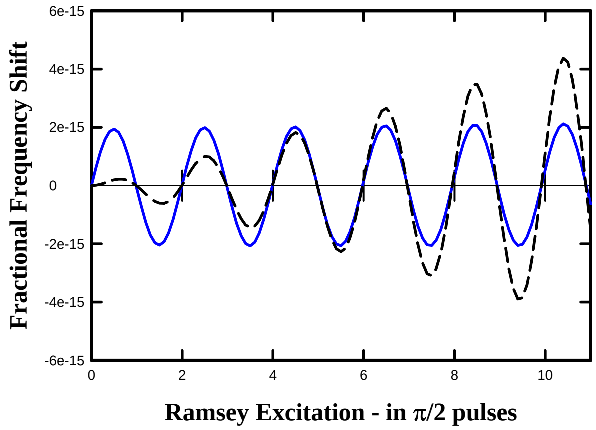

Figure 3. The modeled frequency shift induced by leakage above the Ramsey cavity in NIST-F1 and IEN-CSF1. The solid curve is the case where the leakage amplitude is constant while the field in the Ramsey cavity is increased. The broken curve is the case where the leakage field amplitude is proportional to the amplitude of the field within the Ramsey cavity. The microwave leakage power of each curve was been chosen for convenience and has no particular significance.

5. MICROWAVE LEAKAGE BETWEEN THE TWO RAMSEY PULSES

The dependence of the frequency bias on the amplitude of the microwave field in the Ramsey cavity is shown in Fig 3. It is immediately apparent that the frequency bias caused by microwave leakage is zero at integer multiples of the optimum excitation amplitude, $b_0\tau = {(2n+1)\pi}/{2}$, n=0,1,2... . A measurement of the residual frequency bias can be obtained with some

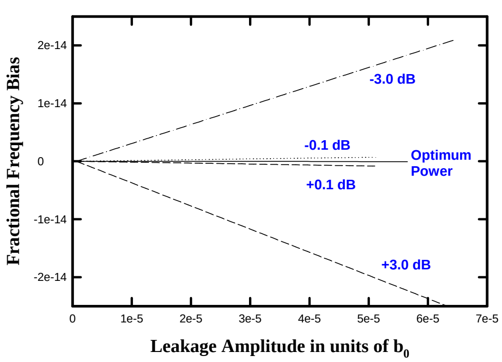

Figure 4. The frequency bias from microwave leakage above the Ramsey cavity can be measured in a "leveraged" fashion by operating well away from optimum microwave power in the Ramsey cavity. Assuming that the normal operating conditions keep the microwave power within 0.1 dB of optimum, a leverage of about 30 can be obtained by operating 3 dB above or below optimum instead.

leverage by measuring well away from optimum power, as illustrated in Fig. 4. In NIST-F1 the microwave power is set to within ± 0.1 dB of optimum, denoted by the dotted lines in Fig. 4. The frequency shift induced by microwave leakage at ± 3 dB from optimum excitation is some 30 times greater than the shift expected within 0.1 dB of optimum. The measurement at ± 3 dB therefore gives a "leverage" of 30 over the standard operating conditions, at least for the specific case of leakage above the Ramsey cavity.

6. MICROWAVE LEAKAGE AFTER THE RAMSEY INTERACTION

In the case of both NIST-F1 and IEN-CSF1 this is the most likely location for microwave leakage to interact with cesium atoms. The power dependence of this shift is shown in Fig. 5. The behavior of this shift is distinct from that caused by leakage above the Ramsey cavity in that its frequency with respect to the Rabi frequency is half that of the case of leakage above the Ramsey cavity. This signature can be used to identify the source of a frequency bias as being caused by leakage either above or below the Ramsey cavity. Unfortunately this shift is difficult to distinguish from the frequency shift caused by distributed cavity phase, as shown in Fig 6. Various approaches to separate these two effects are discussed in [22].

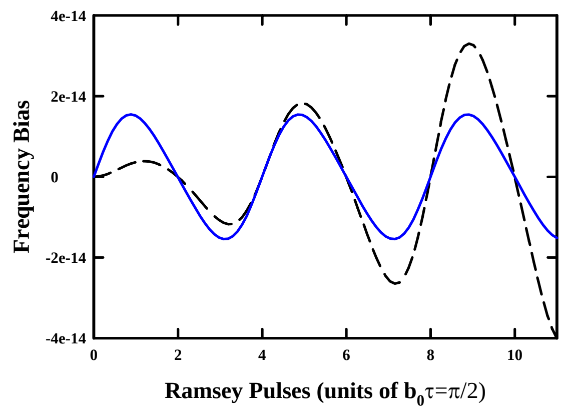

Figure 5. The modeled frequency bias induced by leakage below the Ramsey cavity. The solid curve is the case where the leakage amplitude is constant while the field in the Ramsey cavity is increased. The broken curve is the case where the leakage field amplitude is proportional to the amplitude of the field within the Ramsey cavity. In both cases the microwave power level has been chosen purely for convenience and has no particular significance.

7. DISCUSSION

The frequency biases caused by distributed cavity phase and microwave leakage have distinct signatures when measured as a function of the amplitude of the microwave excitation in the Ramsey cavity. The various shifts can be measured and either "fixed" by eliminating the source of the leakage (best), or perhaps calibrated and corrected.

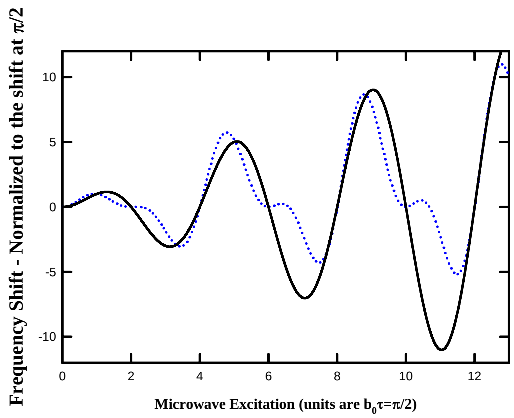

Figure 6. A comparison of the power dependence of the shift caused by microwave leakage (dotted curve) and the shift caused by microwave leakage below the Ramsey cavity (solid curve) as a function of the microwave excitation of the atoms in the Ramsey cavity.

It has been assumed here that the leakage terms must be treated in the small detuning limit. Various other approaches such as using the nonresonant AC Stark shift have been applied to the case of microwave leakage in a cesium fountain [23]. We hold that these cases are not valid approximations in a cesium fountain; the Doppler shift caused by atomic motion is, at 100 Hz maximum, much too small to be considered within the framework of an off-resonant AC Stark shift. The frequency shift caused by microwave leakage in a fountain depends on the amplitude of the microwave field and not on the power (square of the amplitude).

ACKNOWLEDGEMENTS

The authors gratefully acknowledge many useful discussions of microwave field effects in primary frequency standards with Andrea DeMarchi, Bob Drullinger, Bill Klipstein, Stefania Romisch and Tom Parker. We also thank David Smith, Mike Lombardi and Mark Weiss for their many useful suggestions on the manuscript.

REFERENCES

[1] N. Ramsey, Molecular Beams, Oxford – Clarendon Press 1956.

[2] R.C. Mockler, *"Atomic Beam Frequency Standards"*, Adv. Electron El. Phys., **15** (1962) pp.1-72.

[3] S. Jarvis Jr., "Molecular Beam Tube Frequency Biases due to Distributed Cavity Phase Variations", NBS Tech. Note 660 (1975).

[4] A. DeMarchi, J.H. Shirley, D.J. Glaze, and R.E. Drullinger, *"A New Cavity Configuration for Cesium Beam Primary Frequency Standards"*, IEEE Trans. Instrum. Meas. **37** (1988) pp. 185-190.

[5] A. Bauch, B. Fischer, T. Heindorff and R. Schröder, "Performance of the PTB reconstructed primary clock CS1 and an estimate of its current uncertainty", Metrologia **35** (1998) pp. 829-845.

[6] K. Dorenwendt and A. Bauch, "Spurious Microwave Fields in Caesium Atomic Beam Standards: Symmetry Considerations and Model Calculations", Proc. EFTF, 1999.

[7] B. Boussert, G. Théobald, P. Cérez and E. deClercq, *"Frequency Shifts in Cesium Beam Clocks Induced by Microwave Leakages"*, IEEE Trans. UFFC **45** (1998)728-738.

[8] M. Abgrall, "Evaluation des Performances de la Fontaine Atomique PHARO, Participation à l'étude l'horloge spatiale PHARO", PhD Thesis, University de Paris VI, January 2003.

[9] A. DeMarchi, "The Optically Pumped Caesium Fountain: 10^{-15} Frequency Accuracy?", Metrologia **18** (1982) pp. 103-116.

[10] G. Vecchi, A. DeMarchi, "Spatial Phase Variations in a TE_{011} Microwave Cavity for use in a Cesium Fountain Primary Frequency Standard", IEEE Trans. Instrum. Meas. **42** (1993) pp. 434-438.

[11] A Khursheed, G. Vecchi, A. DeMarchi, "Spatial Variations of Field Polarization in Microwave Cavities: Application to the Cesium Fountain Cavity", IEEE Trans UFFC. **43** (1996) pp. 201-210.

[12] S.R. Jefferts, R.E. Drullinger and A. DeMarchi, *"NIST Cesium Fountain Microwave Cavities"*, Proc. 1998 Intl. Freq. Cont. Symp. pp. 6-8.

[13] P. Laurent et al., *"Interrogation of Cold Atoms in a Primary Frequency Standard"*, Proc. 1999 Joint Mtg. IEEE Intl. Freq. Cont. Symp. and EFTF Conf. pp. 152-155.

[14] C. Fertig, R. Li, J. Rees, K.Gibble, "Distributed Cavity Phase Shifts and Microwave Photon Recoils", Proc. 2002 IEEE Intl. Freq. Cont. Symp. pp. 469-472.

[15] G.J. Dick, W.M. Klipstein, T.P. Heavner, S.R. Jefferts, "Design Concept for the Microwave Interrogation Structure in PARCS", Proc. 2003 Joint Mtg. IEEE Intl. Freq. Cont. Symp. and EFTF Conf. pp. 1032-1036.

[16] N. Ashby, S. Römisch, S.R. Jefferts, *"Endcaps for TE_{011} Cavities in Fountain Frequency Standards"*, Proc.

2003 Joint Mtg. IEEE Intl. Freq. Cont. Symp. and EFTF Conf. pp. 1076-1083.

[17] Robert E. Collin, Foundations of Microwave Engineering, 2nd Ed.,McGraw-Hill 1998.

[18] J.H. Shirley, *"Some Causes of Resonant Frequency Shifts in Atomic Beam Machines I. Shifts Due to Other Frequencies of Excitation"*, J. Appl. Phys. **34** (1963) pp.783-788.

[19] J.H. Shirley, *"Solution of the Schrödinger Equation with a Hamiltonian Periodic in Time"*, Phys. Rev. **138** (1965) pp. B979-B987.

[20] J.H. Shirley, W.D. Lee, R.E. Drullinger, *"Accuracy Evaluation of the Frequency Standard NIST-7"*, Metrologia **38** (2001) pp. 427-458.

[21] S.R. Jefferts, J.H. Shirley, N. Ashby, E.A. Burt, G.J. Dick, *"Power Dependence of Distributed Cavity Phase Induced Frequency Biases in Atomic Fountain Frequency Standards"*, IEEE Trans UFFC, in press.

[22] F. Levi, J. Shirley, S.R. Jefferts, *Microwave Leakage Induced Frequency Shifts in the Primary Frequency Standards NIST-F1 and IEN-CSF1, to be submitted.*

[23] K. Szymaniec, W. Chalupczak, P.B. Whibberley, S.N. Lea, D. Henderson, *Evaluation of the Primary Frequency Standard NPL_CsF1*, Metrologia 42 (2005) pp. 49-57.